Multipoint correlators in multifield cosmology

George Panagopoulos and Eva Silverstein

March 17, 2020

Abstract

Connected N-point amplitudes in quantum field theory are enhanced by a factor of $N!$ in appropriate regimes of kinematics and couplings, but the non-perturbative analysis of this for collider physics applications is subtle. We resolve this question for N-point correlation functions of cosmological perturbations in multifield inflation, and comment on its application to primordial non-Gaussianity. We find that they are calculably $N!$-enhanced using a simple model for the mixing of the field sectors which leads to a convolution of their probability distributions. This effect leads to model-dependent but interesting prospects for enhanced observational sensitivity.

Contents

1 Introduction

The behavior of multi-point correlation functions and S-matrix amplitudes at large particle number is of interest for various applications. At tree-level, there is an $N!$ enhancement of large N N-point correlation functions in perturbative quantum field theory as initially studied by Voloshin in [1] and developed by many authors [2] [3] [4] [5] [6].

For S-matrix amplitudes that produce N outgoing quanta, this occurs because the contributions from low-order interaction vertices build up many tree diagrams, of order $N!$. For some regimes of couplings and kinematics, this enhancement is known to survive the sum over tree diagrams (which can be derived equivalently from the classical field configuration) and to persist in the presence of sufficiently small quantum corrections. The interaction probability – obtained by squaring the amplitude and integrating over final particle momenta – contains one $N!$ in the denominator in the phase space for identical particles, leaving a net enhancement. For example, in $\lambda\phi^4$ theory, the $1 \to N$ amplitude near threshold is of order $\lambda^{N/2}N! + \text{loops}$, and the decay probability is of order $\lambda^N N! + \text{loops}$.

In the setting of particle decays and scattering it is not clear to what extent this effect survives in the quantum theory when λN is not perturbatively small. As noted in [5], if it did persist it would have dramatic implications for Higgs physics, leading to a large decay width for the Higgs: the Higgs would fail to be a good quasiparticle at a relatively low energy scale. More recent analyses [7] do not obtain such growth in somewhat similar quantities; still, by investigating this they uncover an interesting emergent 'tHooft expansion arising from a semi-classical approximation, related to results in large-charge quantum field theory [8]. From this perspective, it seems interesting in contrast that we will find a positive result for factorial growth in the setting of early universe cosmology, where the required calculations are actually easier to control.

In time-dependent backgrounds, such as that arising in early universe cosmology, we may ask a similar question for $0 \to N$ processes. A prime example is the set of connected N-point in-in correlation functions relevant for studies of primordial non-Gaussianity, the moments of the probability distribution for scalar fluctuations. The main object of interest there is the wavefuntion of primordial perturbations which seed the structure in the universe. We may write it schematically as

$$\Psi(\zeta(\mathbf{x}), \gamma(\mathbf{x}), \{\chi(\mathbf{x})\}; \{\lambda\}) \tag{1}$$

where ζ and γ are the scalar and tensor perturbations, $\{\chi\}$ represents additional sectors of fields not directly observable, and $\{\lambda\}$ denotes the parameters (couplings) of the theory that generates the perturbations. The probability distribution for the observables ζ, γ is derived from this by tracing over the χ sector,

$$\mathcal{L}(\zeta(\mathbf{x}), \gamma(\mathbf{x})|\{\lambda\}) = \mathrm{Tr}[\rho|\zeta\gamma\rangle\langle\zeta\gamma|] = \int D\chi|\Psi|^2, \quad \rho = \mathrm{Tr}_\chi[|\Psi\rangle\langle\Psi|]. \tag{2}$$

Observations indicate that this is at least approximately Gaussian [10]. A Gaussian distribution arises in free field theory when the system starts in its ground state (or any other Gaussian initial state). In any other situation, the state is non-Gaussian at some level. For a perturbative quantum field theory, the non-Gaussianity vanishes in the limit of zero couplings $\{\lambda\} \to 0$. But for mildly perturbative couplings (such as those arising in particle physics at appropriate scales, with $\lambda \sim 10^{-2}$), the effects of interactions are not arbitrarily small and it is interesting to compute their effects and constrain them with data as systematically as possible.

In situations where the quantum fields in the early universe interact arbitrarily weakly, one can immediately characterize this via low-point correlation functions. These are already rich with different possible shapes in kinematic space [9, 10] which encode various aspects of the dynamics. However, even within the class of field theories with perturbative couplings $\lambda < 1$, interaction effects can build up during inflation [12][13][14] and reheating [15]. This in turn can lead to non-Gaussianity that is not well captured by the lowest-point correlation function [14][15][16][17][18][19].[1]

[1] See also [20] for an interesting analysis of multifield evolution beyond the observable

The structure of the paper is as follows: After explaining qualitatively why the $N!$ enhancement is tractable in dS space in Section 2, we present the methods in detail in section 3. We then present the enhancement for a toy theory that is fully solvable, and prove it for a large class of theories in section 4. In section 5, we investigate implications of this for primordial non-Gaussianity searches, and in section 6 we summarize and mention directions for further research.

2 Simplifications of dS space and local non-Gaussianity

It is perhaps surprising that we are able to derive a general $N!$ enhancement for correlation functions in an inflationary setting while no such result exists for Minkowski space. The results on Minkowski space are accessible in specific regimes of coupling and kinematics in the theory of interest. For example, [1] focuses on $\lambda\phi^4$ and [4] on the weak-coupling multi-particle limit $\lambda n \to \epsilon$, with λ being the coupling, n the number of particles produced and ϵ fixed.

The simplicity of dS space comes in the freezing out of the modes after horizon crossing. In the multifield context, there remains meaningful dynamics outside the horizon, and the dilution of gradients enables the stochastic approach to inflation [11][12] which descends from the full quantum theory as in [13]. Those approaches are able to resum some of the loop contributions by exploiting the fact that $-k\eta \ll 1$, where $\eta \sim -e^{-Ht}/H$ is the proper time which decays at late time exponentially in FRW time t. In QFT in Minkowski space, one has much less control over the loop effects that could spoil the tree-level enhancement of the correlation functions. That is why specific regimes of the phase-space were enforced by hand in the initial investigations of the flat spacetime problem. In the cosmological case, the accelerated expansion itself restricts the phase space naturally.

This is not the first time this phenomenon of a greater simplicity in de Sitter than in flat spacetime has arisen. It has even made an appearance in rigorous mathematics (related to physics): the proof of stability of Kerr black holes [21] pertains in de Sitter spacetime but not otherwise. This is for a similar reason, involving the dilution of perturbations from the accelerated expansion.

The multifield inflationary scenarios that generate local non-Gaussianity captures this simplicity. It enables us to analyze large tails of the primordial scalar perturbations in a controlled way [17]. After the exit from inflation and all the long modes are frozen out, we mix the additional field sectors with the inflaton. As we will see, in the mixing, dS helps us again by suppressing the momentum conjugate to the inflaton by a^3 and enabling us to write the wavefunction evolved by the mixing Hamiltonian as a simple shift in field space.

It would be interesting to explore whether single-field inflationary perturbations can produce the same N!-enhanced correlation functions that we find

horizon and its relation to multipoint correlators and local inferences.

here[2]. There, correlation functions would go like (assuming the tree diagrams constructively add up)

$$\langle \zeta_1 \cdots \zeta_n \rangle \sim N! \lambda^{\alpha N} (1 + c_1 \lambda^\beta N^2 + \dots) \tag{3}$$

with α and β being constants depending on the order of the interaction and λ a dimensionless coupling constant. For example, for a cubic interaction, $\alpha = 1$ and $\beta = 2$, and for a quartic interaction, $\alpha = \frac{1}{2}$ and $\beta = 1$. The leading loop effects come from joining any 2 lines with a propagator, and any two lines at a point respectively. These loop effects can be very large and require resumming. For $\lambda\phi^4$ in some regimes, previews work [4] was able to resum the contributions controlled by λN^2, relegating the question to the effect of those controlled by λN. Even those may be calculable, although this case seems more similar to the particle physics case ([7] versus [5]), something that would be interesting to generalize to cosmological correlators. We will leave this to future work.

3 General Setup and Methods

Observations of cosmological scalar[3] perturbations $\zeta(\mathbf{x})$ may be compared to those predicted by a theoretical probability distribution depending on some parameters $\{\lambda\}$. The likelihood, or probability of the data given the theory, is given by squaring and tracing over the non-observable fields as in (2):

$$\mathcal{L}(\zeta(\mathbf{x})|\{\lambda\}) = \int D\chi |\Psi(\zeta(\mathbf{x}), \chi(\mathbf{x}); \{\lambda\})|^2. \tag{4}$$

Ideally we would compute this functional theoretically, and compare it to data directly. At CMB scales, we would evaluate it on the map; large scale structure may enable a volume's worth of data points, and in [17] we were led to shorter-scale probes. This determines whether, according to the theory, the data is higher-probability with null values $\{\lambda\} = 0$ or for some nonzero values of the couplings (and with what significance). That is not always tractable, so it is useful to work with other quantities derived from the full likelihood.

The set of connected correlation functions of ζ is a useful quantity, which is sometimes easier to compute than the full probability distribution. These are generated by $W(J)$, defined by

$$e^{W(J)} = \int D\zeta e^{\int J\zeta} \mathcal{L}(\zeta|\{\lambda\}) \tag{5}$$

by taking N functional derivatives with respect to J:

$$\langle \zeta_{\mathbf{k}_1} \dots \zeta_{\mathbf{k}_N} \rangle_C = \frac{\delta^N}{\delta J_{\mathbf{k}_1} \dots \delta J_{\mathbf{k}_N}} W(J) \Big|_{J_{\mathbf{k}_i}=0} \tag{6}$$

[2]This goes beyond the low-point functions analyzed in e.g. [22][23][24]) following early work including [11][25].

[3]From now on we suppress the tensor perturbations, which have not been detected at least as of this writing. However, our analysis can be straightforwardly generalized to include tensor modes.

setting J to zero at the end. We will find that these connected correlators scale like $N!$ in a wide class of inflationary scenarios with at least one additional light field. In some cases, there is also an exponential enhancement $\sim \lambda_r^N$, with λ_r a ratio of couplings in the model.

To simplify the analysis, we will often work with another quantity derived from the full likelihood – the histogram of temperature fluctuations, also known as the one-point probability density function. Given a realization of the field, we can count points with a given fluctuation $\hat{\zeta}$:

$$N_{\hat{\zeta}} = k_{\rm max}^3 \int d\mathbf{x}' \delta(\zeta(\mathbf{x}') - \hat{\zeta}) \tag{7}$$

where $1/k_{\rm max}$ is the resolution of the survey, which for simplicity is assumed to be uniform. We can compare this to the average of the histogram according to the field-theoretic distribution (4), given by

$$\langle N_{\hat{\zeta}} \rangle = k_{\rm max}^3 \int d\mathbf{x}' \int D\delta\zeta(\mathbf{x}) \mathcal{L}(\zeta(\mathbf{x})|\{\lambda\}) \delta(\zeta(\mathbf{x}') - \hat{\zeta}) \tag{8}$$

This is the probability of measuring a given value of ζ, $\hat{\zeta}$ at one point, having traced out the field at other points. It can also be used to calculate the N point functions at a single point. In scenarios containing one or more additional light non-shift-symmetric fields present during inflation, this theoretical averaged histogram is determined by a combination of the stochastic methods of Starobinsky as in [12], and the mixing between field sectors. In different regimes one or the other of these may be relevant. We will review this and make use of it below.

3.1 Local non-Gaussianity

A standard form of non-Gaussianity with amplitude parameterized by $f_{\rm NL}^{\rm local}$ is sensitive to the presence of one or more additional fields χ. If these are light, they develop a variance during inflation similar to that of the inflaton perturbations $\delta\phi$. But unlike the inflaton field, their super-horizon interactions are not constrained by symmetries, and they may imprint nonlinearities on the scalar perturbations via a variety of mechanisms [15][26]. Their evolution outside the horizon is ultralocal, as we will review shortly. At the level of the bispectrum, the local shape of non-Gaussianity, which contains correlations between long and short modes, can only be generated if at least one additional field is present [22][24].

In this section, we will set up a class of models of this kind and determine the relative importance of the bispectrum versus other aspects of the distribution, including the power spectrum and higher point correlators. We will make some special choices in specifying the scenario in order to make the calculations as simple as possible. After deriving the factorial enhancement explicitly in a simple example, we will show that it extends to a much wider class of models.

Consider a system with two fields, the inflaton ϕ and another scalar χ. We denote the wave functional of the perturbations $\delta\phi(\mathbf{x})$ and $\chi(\mathbf{x})$ as $\Psi(\delta\phi(\mathbf{x}), \chi(\mathbf{x}), t)$;

we will eventually trace out χ because $\zeta \sim H\delta\phi/\dot{\phi}$ will be the directly observed scalar perturbation. We are interested for simplicity in cases where the scalar perturbation is dominated by the mostly-Gaussian fluctuations of $\delta\phi$, but where there is an additional, potentially very-non-Gaussian contribution, which will dominate in higher-N N-point functions of $\delta\phi$. This is somewhat analogous to the cases in [14], although the origin of the enhanced non-Gaussianity will be different (coming from factorial enhancements of connected correlation functions). As above, the probability distribution at time t_0 will be given by the functional integral

$$P(\delta\phi) = \int D\chi |\Psi(\delta\phi, \chi, t_0)|^2 = \mathrm{Tr}[\rho|\delta\phi\rangle\langle\delta\phi|] \tag{9}$$

where $\rho = \int D\chi |\Psi\rangle\langle\Psi|$ is the density matrix obtained by tracing out χ.

There is a wide range of initial conditions that lead to inflation; see [27, 28] for some recent developments. However, we will simply start from the Bunch-Davies vacuum. This is a conservative choice for our purposes, as it avoids introducing non-Gaussianity at the level of the initial state. We would like to understand the possible N! enhancement of $0 \to N$ processes in the time dependent background, so we start in the vacuum, with no particles in the initial state.

To separate issues we will prescribe various time-dependent couplings which can be mediated by fields that evolve outside the horizon, e.g. at reheating, as discussed extensively in the early literature on multifield inflation and non-Gaussianity such as [26]. In particular, we will introduce mixing between χ and $\delta\phi$ after they have evolved independently over $\sim N_e$ e-foldings.

To begin, for each mode k, there is a time $t_{c,k} \sim \log(k/k_*)/H$ at which it has just exited the horizon. Let us denote by t_c the time at which all modes accessible in the CMB have exited the horizon. At this time, as just mentioned, we have a direct product state

$$\Psi(\delta\phi, \chi, t_c) = \psi_G(\delta\phi, t_c)\psi_\perp(\chi, t_c) \tag{10}$$

where we are neglecting slow-roll corrections and hence ψ_G is the approximately Gaussian state of the inflaton fluctuations, of the form

$$\psi_G(f) \sim \sqrt{\det(C)}\exp(-fC^{-1}f) \tag{11}$$

with covariance matrix

$$C \sim \delta(\mathbf{k} + \mathbf{k}')P_{\delta\phi}(k), \qquad P_{\delta\phi}(k) \sim \frac{H^2}{k^3} \tag{12}$$

encoding scale invariant perturbations.

There are in principle many choices for the state of the transverse sector and its dynamics. We will consider a light field χ, of mass $m_\chi \ll H$, starting in its ground state. For the full range of χ , we take its potential energy $V(\chi)$ to be subdominant to the inflaton potential in sourcing inflation; the slow roll

conditions are satisfied separately in the χ directions. The interactions in the χ sector build up over a large number of e-foldings N_e, with each mode outside the horizon affected by a stochastic distribution of shorter modes [12][11]. In the next section, we will illustrate this buildup of nonlinearities. In some cases we may focus on the late-time limit, and its equilibrium 1-point probability distribution. Here each 'point' is a patch of size the correlation length, R_S described below, and the distribution obtained by tracing over the other patches is the equilibrium solution to the appropriate Fokker-Planck equation [12]

$$\int D\chi(x \neq x_0)|\Psi_\perp(\chi)|^2 \to \rho_{eq} \sim \mathcal{N}_{eq} e^{-4\pi^2 V(\chi(x_0))/3H^4} \tag{13}$$

where $\mathcal{N}_{eq}$ is a normalization factor. This was worked out in detail, with a focus on the $\lambda\chi^4$ theory in [12]. Subleading corrections to this classical stochastic approximation and its derivation from the full quantum field theory were examined in [13].

Similar results hold for multiple χ fields, and other potentials, but with an interesting subtlety. To explain what we mean by this, let us focus on potentials of the form

$$V(\chi) = \mu^{4-p}|\chi|^p \tag{14}$$

This is a particular family of models motivated by the potential-flattening effects of multiple, generically massive, fields as we review further below [29]. The behavior at the origin in (14) may be smoothed out by integrating in additional fields, but for the present discussion this will not be necessary and in fact the form (14) leads to a very simple analysis.

The Fokker-Planck equation for the one-point pdf of the long modes of χ takes the form

$$\frac{\partial \rho_1}{\partial t} = \frac{H^3}{8\pi^2}\frac{\partial^2 \rho_1}{\partial \chi^2} + \frac{1}{3H}\frac{\partial}{\partial \chi}\left(V'(\chi)\rho_1\right) \tag{15}$$

The equilbrium solution arises from setting $\partial\rho_1/\partial t = 0$. To capture the approach to equilibrium (when it pertains), we need more general solutions. It is useful to work as reviewed in [17] in a basis of eigenstates of the operator on the right hand side, which gives an analogue Schrodinger problem [12]

$$\left(-\frac{\partial}{\partial\chi^2} + [v'(\chi)^2 - v''(\chi)]\right)\Phi_n(\chi) = \left(-\frac{\partial}{\partial\chi} + v(\chi)\right)\left(\frac{\partial}{\partial\chi} + v(\chi)\right)\Phi_n(\chi) = \frac{8\pi^2\Lambda_n}{H^3}\Phi_n(\chi) \tag{16}$$

with $v(\chi) = 4\pi^2 V(\chi)/3H^4$. The effective potential $w(\chi) \equiv v'(\chi)^2 - v''(\chi)$ in this problem leads to a vanishing lowest eigenvalue, $\Lambda_0 = 0$; this corresponds to the solution $\propto e^{-v(\chi)}$ (13) as can be seen immediately from the middle form of (16). When the nonzero eigenvalues $\Lambda_{n>0}$ are gapped, as we approach equilibrium the non-equilibrium terms are suppressed exponentially, $\sim e^{-\Lambda_n(t-t_0)}$.

In the family of models (14), the effective Schrodinger potential $w(\chi)$ has a delta function potential well at the origin which holds the ground state (or a smoothed version with Λ_* turned on). (This comes from the $v''(\chi)$ term, with the derivatives acting on the cusp at the origin.) For $p > 1$, $w(\chi) \to \infty$ as

$|\chi| \to \infty$ and the energy levels are discrete. For $p = 1$, $w(\chi)$ approaches a positive constant at large field values: there is a continuum above a gap, with $\Lambda_{gap}/H \sim (\mu/H)^6$. For $p < 1$, $w(\chi) \to 0$ as $|\chi| \to \infty$, leading to an ungapped continuum of excited states. It is straightforward to verify in this formalism that the $p = 0$ case reproduces free field theory fluctuations.

3.2 Mixing with ϕ and the probability distribution for ζ

Finally at a late time t_0, to convert χ to $\delta\phi$, we introduce a mixing interaction

$$\mathcal{S}_{mix} = \int dt \int d\mathbf{x}\, a(t)^3 F_{mix}(\chi)\dot{\phi}^2 \tag{17}$$

with support between times t_0 and $t_0 + \Delta t$. We can understand the effect of this interaction by noting that during inflation, $\dot{\phi} = \dot{\overline{\phi}}(t) + \delta\dot{\phi}(\mathbf{x}, t)$, where the first term is the leading homogeneous piece. Thus, the interaction is, to leading order

$$\mathcal{S}_{mix} \sim \int dt \int d\mathbf{x}\, \dot{\overline{\phi}}[a(t)^3 \delta\dot{\phi}] F_{mix}(\chi) \tag{18}$$

We can write this in terms of the conjugate momentum to the inflaton fluctuation $\delta\phi$, $\Pi_{\delta\phi} = a(t)^3\delta\dot{\phi}$ leading to a mixing Hamiltonian

$$H_{mix} = \int d\mathbf{x}\, \dot{\overline{\phi}}\, \Pi_{\delta\phi} F_{mix}(\chi) \tag{19}$$

that dominates over the free Hamiltonian, as described in [17]; for completeness we briefly summarize the setup here. The operator $\Pi_{\delta\phi}$ is the generator of translation in field space and so the evolution over Δt is just a shift of the wavefunction:

$$\Psi(\chi, \delta\phi, t_0 + \Delta t) = \Psi(\chi, \delta\phi + \dot{\overline{\phi}}\Delta t F_{mix}(\chi), t_0) \tag{20}$$

Putting all this together, the likelihood for $\delta\phi \sim \zeta\dot{\phi}/H$ is then given to good approximation by

$$\mathcal{L}(\delta\phi|\{\lambda\}, \kappa) = \int D\chi_0\ |\psi_\perp(\chi_0, t_0)|^2\ |\Psi_G(\delta\phi + \kappa F_{mix}(\chi_0))|^2 \tag{21}$$

up to $1/N_e$ corrections. Here we have defined $\kappa \equiv \dot{\overline{\phi}}\Delta t$. After this step of evolution, we postulate that reheating quickly leads to a local thermal distribution, with $\delta\phi \sim \zeta\dot{\phi}/H$ distributed according to the likelihood (21). Given this, ζ remains constant during the remaining evolution outside the horizon, and (21) contains the primordial non-Gaussianity.

For the case where we reach the equilibrium distribution in the χ sector, the one-point pdf for $\delta\phi$, defined as in (8), is easily computed by Gaussian integration

$$\langle N_{\delta\hat{\phi}} \rangle = \int d\vec{\chi}_0\, \mathcal{N}_{eq} \exp(-4\pi^2 V(\vec{\chi}_0)/3H^4) \frac{\exp(-(\delta\hat{\phi} + \kappa F_{mix}(\vec{\chi}_0))^2/2\sigma^2)}{\sqrt{2\pi}\sigma}\ , \tag{22}$$

where we used (13), and we have allowed for the possibility of multiple χ fields. Here the width σ is given by

$$\frac{1}{2\sigma^2} = C^{-1}_{x',x'} + 4C^{-1}_{x',\perp}(C^{-1}_{\perp,\perp})^{-1}C^{-1}_{\perp,x'} \tag{23}$$

where C is the covariance matrix in position space, and $\perp$ denotes points not equal to x'. This width is of order H. Again, (23) can be traded for the $\hat{\zeta} \sim H\delta\hat{\phi}/\dot{\phi}$ histogram.

3.3 Regime of applicability of the equilibrium distribution

Let us now spell out the regime of applicability of the equilibrium distribution. This depends in part on the relative size of various relevant patches.

In the derivation of the equilibrium distribution, following [12] let us denote the correlation length as

$$R_S \sim H^{-1}e^{H/\Lambda_1}. \tag{24}$$

As reviewed in [17], this can be read off from the two point correlation function.

We must compare this to two other scales. First, we have the size of the observable patch of the universe,

$$R_{obs} = \frac{1}{H}e^{n_e} \tag{25}$$

where $n_e < 60$ is the total number of efoldings of phenomenological inflation. The third scale of interest is the scale of resolution of the CMB, or of some shorter-scale probe such as PBHs. This we will parameterize as

$$R_{res} \sim \frac{1}{H}e^{n_e-\Delta n_e} \tag{26}$$

The number of independent patches is

$$N_P = \left(\frac{R_{obs}}{R_S}\right)^3 \tag{27}$$

To have more than one patch in the observable universe, each of which larger than the resolution, we need

$$e^{n_e-\Delta n_e} < R_S H < e^{n_e} \tag{28}$$

In other words, the equilibrium distribution applies in a straightforward way for

$$\frac{1}{n_e} < \frac{\Lambda_1}{H} < \frac{1}{n_e - \Delta n_e} \tag{29}$$

where the eigenvalues Λ_n depend on the model parameters as determined by (16). For example, for the $p = 1$ model $V(\chi) = \mu^3\chi$ we find $\frac{\Lambda_1}{H} \sim \frac{\mu^6}{H^6}$, while for the $p = 4$ model $V(\chi) \sim \lambda\chi^4$ we have $\frac{\Lambda_1}{H} \sim \sqrt{\lambda}$ [12].

If we restricted attention to the CMB, then this particular scenario, with the χ sector reaching the equilibrium distribution, pertains for a rather particular value of the coupling in this family of models (although one which might arise in a rich potential landscape). Moreover, once it reaches equilibrium, the contribution χ makes to the fluctuations is very blue. For shorter scale probes, such as primordial black holes, there is a wide window of applicability as described in [17]. However, at least in that context the stochastic evolution of χ is only applicable to the leading observables if the potential drifts outward, for reasons explained in [17]. As we will review further below, the mixing interaction itself can introduce strong non-Gaussianity associated with the tail of the distribution.

3.4 Flattened directions in field space and Non-Gaussian tails

The effect of $\vec{\chi}$ on the histogram for $\delta\hat{\phi}$ can be understood analytically to some extent. We will be particularly interested in the tails of the distribution. To see whether or not the Gaussian tail dominates for $\delta\hat{\phi} \gg H$, consider field configurations where the Gaussian suppression is canceled by the $\vec{\chi}_0$ field:

$$F(\vec{\chi}_{0,tail}) \simeq -\delta\hat{\phi}/\kappa. \tag{30}$$

In that regime, the probability is suppressed by $\exp(-4\pi^2 V(\vec{\chi}_{0,tail})/3H^4)$. If in this direction (or directions) in field space, the potential $V(\vec{\chi}_{0,tail})$ is flatter than quadratic in $\delta\hat{\phi}$, then the Non-Gaussian tail dominates over the Gaussian at sufficiently large $\delta\hat{\phi}$. In order to be potentially observable, the overall probability of this tail must be larger than $1/N_P$ where N_P is the number of independent data points in the survey volume: roughly,

$$\int_{tail} d\delta\hat{\phi} \frac{\mathcal{N}_{eq}}{\sqrt{2\pi}} \exp(-4\pi^2 V(\vec{\chi}_{0,tail}(\delta\hat{\phi}))/3H^4) > \frac{1}{N_P} \tag{31}$$

Flattened potentials arise naturally from adjustments of heavier fields as in [29] as well as for other reasons such as those studied in [31][32]. In fact, constraining the Non-Gaussian tail in our scenario gives us a new way to probe large field ranges, in the χ sector rather than the inflaton sector. The less efficient our conversion is (i.e. for smaller mixing κ), the larger the field range is that we probe.[4] Here, we probe the field range via the quantum (effectively stochastic) fluctuations of χ rather than the classical motion of χ, and via non-Gaussianity rather than the tensor to scalar ratio.

Of course, the distributions differ in other ways than asymptotically on the tail. In some cases, including an axionic χ field, the Non-Gaussian histogram contains an intermediate region where it exceeds the Gaussian, before rejoining the Gaussian tail further out. When probability moves to a region away from the origin in $\delta\hat{\phi}$, this is made up by a suppression of probabiliy near the origin.

[4] This is somewhat reminiscent of observations in [26].

Low-point moments are sensitive to the latter effect, and it is a quantitative question to determine which measurements best capture the difference in the two distributions. PBH formation is directly sensitive to the tail, as we analyzed in [17]. But other parts of the distribution may lead to other signals and constraints to take into account. We will comment on this briefly after deriving the factorial enhancement in a wide class of multifield models.

4 The generating functional for connected N-point functions and $N!$ enhancement

One tractable probe of the distribution is its moments, the N-point correlation functions. Also from a purely theoretical point of view, we would simply like to deteremine the fate of the factorial enhancement [1] in our cosmological setting.

We can estimate the N dependence of the N-point functions by first extracting the connected ones by computing the generating functional

$$Z(J) = e^{-W[J]} = \int D\delta\phi \; \mathcal{L}[\delta\phi|\lambda,\kappa] \; e^{-\int J\delta\phi} \tag{32}$$

with the connected N-point function given by

$$\left.\frac{\delta^N W}{\delta J_{\mathbf{k}_1}\dots\delta J_{\mathbf{k}_N}}\right|_{J_{\mathbf{k}_i}=0} \sim \langle\delta\phi_{\mathbf{k}_1}\dots\delta\phi_{\mathbf{k}_N}\rangle_C. \tag{33}$$

and the disconnected diagrams obtained from a similar formula with $W(J)$ replaced with $Z(J)$. For our case, the likelihood takes the special form (21), so we get

$$e^{-W[J]} = \int D\chi_0|\psi_\perp[\chi_0]|^2 \int D\delta\phi P_G[\delta\phi - \kappa F(\chi_0)]e^{-\int J\delta\phi} \tag{34}$$

The path integral over $\delta\phi$ is a Gaussian, and gives

$$e^{-W[J]} \sim e^{JCJ} \int D\chi_0|\psi_\perp[\chi_0]|^2 e^{-\int \kappa JF(\chi_0)} \tag{35}$$

where C is the Gaussian covariance (12). We will discuss saddle point estimates for the χ_0 integral below, working with the 1-point pdf (histogram).

But first, we will derive $W(J)$ for a special choice of $\psi_\perp$ and $F(\chi)$ which is nontrivial but completely calculable in the full quantum field theory. For the transverse state, we will simply take a Gaussian $\psi_G(\chi_0)$ (11). For the mixing interaction, we consider

$$F(\chi_0) = \frac{\chi_0^2}{M} + \chi_0 \tag{36}$$

This form arose from interesting (p)reheating dynamics in [15]. If the mass parameter M is of order H, this is fully nonlinear; the effective coupling is H/M.

4.1 Full field theory calculation in a special case

For this case, the result is

$$W[J] \sim \int d\mathbf{k} d\mathbf{k}' \sqrt{P_{\delta\phi}(k)} J_{\mathbf{k}} \left[\delta_{\mathbf{k},\mathbf{k}'} + \kappa^2 \left(\delta_{\mathbf{k}\mathbf{k}'} + \kappa \frac{J_{-\mathbf{k}+\mathbf{k}'}}{M} \sqrt{P_{\delta\phi}(k) P_{\delta\phi}(k')} \right)^{-1} \right] \sqrt{P_{\delta\phi}(k')} J_{\mathbf{k}'}$$
$$- \frac{1}{2} \mathrm{Tr} \log \left(\delta_{\mathbf{k}\mathbf{k}'} + \kappa \frac{J_{-\mathbf{k}+\mathbf{k}'}}{M} \sqrt{P_{\delta\phi}(k) P_{\delta\phi}(k')} \right) + \text{const} \tag{37}$$

Evaluating the derivatives (33) after expanding $W[J]$ in a power series in J gives us the following result for the N-point function. From the top line of (37) we obtain, for $N > 2$, [5]

$$\langle \delta\phi^N \rangle|_0 \sim \frac{\kappa^N}{M^{N-2}} \delta(\sum \mathbf{k}) P_{\delta\phi}(k_1) P_{\delta\phi}(|\mathbf{k}_1 + \mathbf{k}_2|) P_{\delta\phi}(|\mathbf{k}_1 + \mathbf{k}_2 + \mathbf{k}_3|) \dots P_{\delta\phi}(|\mathbf{k}_1 + \dots + \mathbf{k}_{N-2}|) P_{\delta\phi}(k_N)$$
$$+ \text{permutations}$$
$$\sim \kappa^N N! \tag{38}$$

which has the structure of a tree diagram. From the second line we obtain

$$\langle \delta\phi^N \rangle|_1 \sim \frac{\kappa^N}{M^N} \delta(\sum \mathbf{k}) \int d^3\mathbf{k} P_{\delta\phi}(k) P_{\delta\phi}(|\mathbf{k}_1 + \mathbf{k}|) P_{\delta\phi}(|\mathbf{k}_2 + \mathbf{k}_1 + \mathbf{k}|) \dots P_{\delta\phi}(|\mathbf{k}_{N-1} + \dots + \mathbf{k}_1 + \mathbf{k}|)$$
$$+ \text{permutations}$$
$$\sim \kappa^N N! \tag{39}$$

This has the structure of a loop diagram. These contributions both have the expected scaling with momenta for a nearly scale-invariant theory. The amplitude is enhanced by $N!$. The overall level of non-Gaussianity of the map is naively of order $\frac{\langle \delta\phi(x)^N \rangle_c}{\langle \delta\phi(x)^2 \rangle^{N/2}} \sim N! \kappa^N \left(\frac{H}{M}\right)^{N-2}$ from (38), but this does not generally reflect the actual observable level.

For more general $\psi_\perp(\chi)$ and $F(\chi)$, we can obtain similar results, now using a saddle point approximation to the integral. Shortly we will see that for a rather generic (but not entire) nonlinear function, the order N term in the expansion of $W[J]$ has no factorial suppression. Hence, N-point correlators obtained by Nth functional derivative will be factorially enhanced. To make this clear, we can study a 1d integral version of the problem, the histogram of scalar fluctuations defined above. We will show this in the next subsection.

4.2 More general theories and the factorial enhancement

We would like to understand how general the factorial enhancement is given a more generic model than the one just analyzed. Clearly small perturbations around the example above will not change the conclusion. More generally, we

[5] The N-point functions for ζ are obtained by the rescaling $\zeta \sim H\delta\phi/\dot{\phi}$.

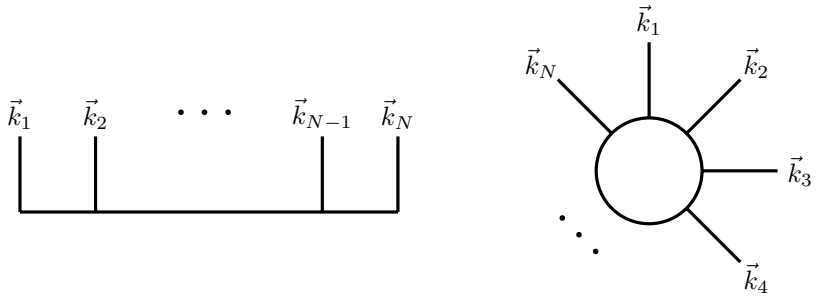

Figure 1: A diagrammatic representation of the two contributions to the N-point function described in the text, (38) on the left and (39) on the right.

can analyze this by considering the histogram version of the integral (35). This suffices to capture the N-point functions at coincident points, and hence it is enough to determine the factorial structure. (However, it does not necessarily capture the strongest tails in the full quantum field theory.) For this exercise, let us consider the histogram arising from the equilibrium distribution [12] discussed above:

$$Z(J) = e^{-W(J)} \sim \int d\vec{\chi}_0 \exp\left(-\frac{4\pi^2 V(\vec{\chi}_0)}{3H^4} - \kappa J F(\vec{\chi}_0)\right). \tag{40}$$

We have not included the $e^{JC^{-1}J}$ term here as it only contributes to the 2-point function, or the normalization since this drops out of the N point function growth. The N-point functions are obtained by taking N ordinary derivatives of $W(J)$, which still captures the combinatorial factors. These depend on the behavior of the coefficients in a series expansion of $W(J)$ (or $Z(J)$ for the disconnected diagrams).

We can assess the combinatorial factor using the structure of the integrals that arise in the expansion with respect to J. The disconnected diagrams are generated by

$$Z(J) = \sum_n z_n \kappa^n J^n \tag{41}$$

The corresponding disconnected N point functions go like $z_N N! \kappa^N$. So these have a factorial enhancement if the coefficients z_n are not suppressed by $1/n!$, in which case the series has a finite radius of convergence (possibly zero, meaning the series is only asymptotic). For that to be the case, the function $Z(J)$ should not be entire. One way that a function can fail to be entire is if it diverges somewhere in the complex κ plane. This in turn depends on whether the potential $V(\vec{\chi}_0)$ grows more quickly than $F(\vec{\chi}_0)$ in every direction in field space. If not, then the disconnected diagrams have a factorial growth, and the distribution has a non-Gaussian tail at sufficiently large $\delta\hat{\phi}$, as discussed above.

For the connected N point functions derived from $W(J)$ we have a similar criterion for a factorial enhancement. This may have an enhancement even when

the disconnected correlators do not (one can see an example of this simply from the fact that taking the logarithm leads to non-analyticity at the zeros of (40)).

We proceed by evaluating the integral by saddle point. The saddle point equation for χ_{0I}^* is:

$$\frac{4\pi^2 \partial_I V(\vec{\chi}_0^*)}{3H^4} + \kappa J \partial_I F(\vec{\chi}_0^*) = 0 \tag{42}$$

It will be useful to express the function F evaluated on the solution to this equation by a power series

$$F(\vec{\chi}_0^*(J)) = \sum_{n=0}^{\infty} a_n J^n \tag{43}$$

The saddle point value of $W(J)$ is

$$W(J) = \frac{4\pi^2 V(\vec{\chi}_0^*)}{3H^4} + \kappa J F(\vec{\chi}_0^*). \tag{44}$$

Differentiating $W(J)$ with respect to J and using (42) we obtain the differential equation

$$\frac{dW}{dJ} = \kappa F(\vec{\chi}_0^*(J)) \tag{45}$$

which upon integration gives

$$W(J) = \kappa \sum_{n=0}^{\infty} \frac{a_n J^{n+1}}{n+1} \tag{46}$$

after we impose that $W(J=0) = 0$. The N-point functions are thus $\sim a_N N!$. The main question is then how the coefficients a_N scale. If they cancel the $N!$ enhancement then clearly the power expansion of $F(\vec{\chi}_0^*(J))$ must converge for all complex J and thus the function must be entire. This is a very stringent requirement and is not true in general.

To simplify the analysis, let us now specialize to the case of a single variable χ_0. Equation (42) can be viewed as an inversion problem. We are given $J = g(\chi_0^*)$, where the function g is

$$g(x) = -\frac{4\pi^2 V'(x)}{3H^4 \kappa F'(x)} \tag{47}$$

and we want to show that $F \circ g^{-1}$ is not entire. Consider, for example, $F(x) \propto x$. Then, a sufficient (but not necessary) condition is that g' has finite roots in the complex plane as that would imply that the derivative of g^{-1} has a pole at that point. Furthermore, for this particle example for F, this corresponds to the question of whether $V''(x)$ has roots in the complex plane.

4.3 Example of non-analytic $W(J)$

It is possible for the saddle point equation to have a solution which is not Taylor expandable. A simple but important example is a potential of the form $V(\chi_0) = |\frac{\chi_0}{M}|^p$, with $p > 1$ and $F(\chi_0) = \chi_0$. The integral is then (neglecting all constants as they can be absorbed in the definition of J)

$$Z(J) = e^{-W(J)} \sim \int_{-\infty}^{\infty} d\chi_0 \exp\left(-|\chi_0|^p - J\chi_0\right) = 2\int_0^{\infty} dx e^{-x^p} \cosh(Jx) \quad (48)$$

To conclude that the connected correlation functions exhibit an $N!$ enhancement, it suffices to show that there exists a $J_0 \in \mathbb{C}$ such that $Z(J_0) = 0$. Then W has a logarithimic branch cut at $J = J_0$ and is thus not analytic everywhere.

To that end, let J be purely imaginary and define $J \equiv iy$. Then,

$$Z(iy) = 2\int_0^{\infty} dx e^{-x^p} \cos(yx) \quad (49)$$

This as a function of y is purely real and continuous. Therefore, if we can prove that it takes a negative value, it would imply that it also has a zero. For concreteness, take $y = 2\pi$

$$Z(2\pi i) = 2\int_0^{\infty} dx e^{-x^p}(1 - 2\sin^2(\pi x)) = 2\Gamma\left(1 + \frac{1}{p}\right) - 4\int_0^{\infty} dx e^{-x^p} \sin^2(\pi x) \quad (50)$$

We can make a series of approximations to the final integral

$$\begin{aligned}\int_0^{\infty} dx e^{-x^p} \sin^2(\pi x) &> \int_0^1 dx e^{-x^p} \sin^2(\pi x) > \int_0^1 dx(1 - x^p)\sin^2(\pi x) \\ &> \frac{1}{2} - \int_0^1 dx x^p \pi^2 (x-1)^2 = \frac{1}{2} - \frac{2\pi^2}{(p+1)(p+2)(p+3)}\end{aligned} \quad (51)$$

to conclude that

$$Z(2\pi i) < 2\Gamma\left(1 + \frac{1}{p}\right) - 2 + \frac{8\pi^2}{(p+1)(p+2)(p+3)} \quad (52)$$

which is negative for $p > 6.4$ and goes as $-\frac{2\gamma}{p}$ for large p.

For values close to $p = 2$, we can numerically Taylor-expand $Z(2\pi i)$ around $p = 2$. This gives

$$Z(2\pi i) \approx 9.17 \times 10^{-5} - 3.85 \times 10^{-2}(p - 2) \quad (53)$$

which is negative for $p > 2.003$. We can fill in the intermediate regime by taking more terms in the approximations above. The result is that $Z(2\pi i)$ is negative for all $p > 2.003$.

5 Comments on observational implications

It is interesting to apply these results to primordial non-Gaussianity searches. It sharpens the question of systematically mapping out the ideal probe of Non-Gaussianity (low point functions versus the histogram or higher moments).[6] In the present context, this may be model-dependent as a result of the exponential dependence of the tail of the distribution on the fields and parameters.

In [17] we focused on primordial black hole production, which occurs on shorter scales than the CMB. In this section, we will consider the histogram (8) which might be applied to the CMB or large scale structure. As described above in section 3.3, the applicability of the stochastic nonlinearities is limited to a narrow (but nonvanishing) window in coupling (29). However, the mixing itself introduces heavy tails of the distribution in appropriate cases, and in those examples there is no such limitation.

5.1 Signal to Gaussian noise formula and its limitations

In the collider physics version of this quantum field theory problem [1][2] [3] [4] [5][7], the quantity of physical interest is the cross section (squared N point function amplitude). This is factorially enhanced at tree level, sufficiently close to threshold. The analogous squared quantity in our case, formally, would be signal to noise estimate for an N point function estimator.

In all examples with a factorial enhancement, the ratio of the non-Gaussian mean and the Gaussian variance, which we review shortly, is similarly factorially enhanced. This by itself would naively indicate a generic new discovery window for non-Gaussianity. However, it is necessary to analyze the full distribution of the estimator to determine how likely such a discovery would be, and this turns out to be model-dependent.

By working in the cosmic variance limited regime of CMB observations, we can focus on the noise introduced by the quantum fluctuations of the fields themselves. In general, this is highly nontrivial, with a covariance matrix

$$C^{(N)}_{\{\mathbf{k}_1,\ldots,\mathbf{k}_N\},\{\mathbf{k}'_1,\ldots,\mathbf{k}'_N\}} = \langle \zeta_{\mathbf{k}_1} \ldots \zeta_{\mathbf{k}_N} \zeta_{\mathbf{k}'_1} \ldots \zeta_{\mathbf{k}'_N} \rangle \tag{54}$$

which is a $2N$-point function.

Including only the noise from Gaussian fluctuations, and including only connected contributions to the N-point functions, this matrix is diagonal and leads to a relatively simple expression

$$\begin{aligned}(S/N)^2 &= \int_{\{\mathbf{k}\},\{\mathbf{k}'\}} \langle \zeta_1 \ldots \zeta_N \rangle^*_C \, C^{(N)}(\{\mathbf{k}\},\{\mathbf{k}'\})^{-1} \, \langle \zeta_{1'} \ldots \zeta_{N'} \rangle_C \\ &\to \int_{\{\mathbf{k}\}} \frac{|\langle \zeta_{\mathbf{k}_1} \ldots \zeta_{\mathbf{k}_N} \rangle_C|^2}{N! \prod P(k_i)} \equiv (S/N)^2_G\end{aligned} \tag{55}$$

[6] As mentioned above, the dominance of higher point functions has arisen previously in examples [15][16][17][18][14][19]. Another previous incarnation of this question led to a negative result in a different context as explained in [33].

where

$$P(k) \sim \frac{H^4}{\dot{\phi}^2 k^3} \tag{56}$$

is the power spectrum for ζ. Here the $N!$ in the denominator compensates for the unrestricted momentum integrals over the N identical fields in the final state This is similar to the $1/N!$ arising in the multiparticle density of states for scattering with identical final particles. The integrals over phase space are restricted to

$$k_{\rm min} < \{|\mathbf{k}|\} < k_{\rm max} \tag{57}$$

where $k_{\rm min} \sim 1/L$ with L the size of the survey, and $k_{\rm max}$ is the largest momentum scale we can probe. One can analyze this quantity, finding that it has an interesting enhancement related to the N! growth of correlators. Nonetheless, the probabilility of a detection for a given N_{pix} is model-dependent within this class. The reason that the nominal S/N is not a good guide is that the distribution of the estimator may be highly non-Gaussian. We see that explicitly below in figure 3.

5.2 Basic estimates of observational sensitivity

One diagnostic of the information available to distinguish the Non-Gaussian probability distribution from the Gaussian one is the relative entropy (also known as the Kullback—Leibler divergence), an average of the log of the ratio of likelihoods at two values of some theoretical parameter λ:

$$\mathcal{S}_{rel} \equiv \int D\zeta P(\zeta) \log\left(\frac{\mathcal{L}(\zeta(\mathbf{x})|\{\lambda\})}{\mathcal{L}(\zeta(\mathbf{x})|\{0\})}\right) \tag{58}$$

Here, $P(\zeta)$ may be taken to be either of the two probability distributions; $\mathcal{S}_{rel}$ is not symmetric. The first term in its Taylor expansion about $\{\lambda\} = 0$ is the Fisher metric $F_{\lambda\lambda}$. As we will see, in some cases, the relative entropy (58) is well approximated by the first term in the Taylor expansion, the constraint on λ is well estimated by the inverse of the Fisher metric, and low-point correlation functions suffice to achieve this constraint. In other cases, this first term is subdominant, and there is more information available (e.g. on the tail of the distribution). Moreover, certain observables (such as primordial black hole production [17]) are specifically sensitive to the tail.

The analysis above establishes factorial enhancement of N point functions for the families of models described above in (59), and it is clear that this extends to many others. We note that the factorial enhancement of the connected diagrams is universal in this class, while that of the disconnected diagrams is model dependent. For example, we can parameterize a class of models by

$$V = \mu^{4-p}(\Lambda_*^2 + \chi^2)^{p/2}, \qquad F(\chi) = H\left(\frac{\chi}{H}\right)^m \xrightarrow[m\to\infty]{} He^{2\chi/M_*} \tag{59}$$

The tail becomes stronger with larger m/p. Small values of p emerge from the flattening mechanism discussed in [29]; moreover, with more generic kinetic

terms, the possibilities proliferate, at least in some cases leading to a flatter distribution for different reasons [31][32]. Large integer values of m do not appear particularly well-motivated a priori, but the $m \to \infty$ limit leads to a Wilsonian-natural model of a hyperbolic field space

$$F(\chi) \sim He^{2\chi/M_*} \tag{60}$$

similar to the structure of the kinetic terms considered in e.g. [34]. As mentioned in [17], this has a very heavy tail compared to the Gaussian case. We can think of the first expression in (59) as an ad hoc parameterization of the slope of the potential in the direction giving the strongest contribution to the tail. In this class, the heavier than Gaussian tails only arise for $p < m$. So for example, the χ^4 theory with mixing $m \leq 4$ has a Gaussian tail asymptotically, but still has factorial-enhanced connected N point functions. One can also analyze fields with an underlying periodicity, something also considered in [19]. In the case (60), the dominant contribution to the non-Gaussianity is from the mixing interaction, liberating us from the condition (29) as anticipated above.

5.2.1 Corrections to the power spectrum ($N = 2$)

Before considering the tail of the distribution, it is interesting to ask what the effect of the mixing is on the power spectrum. At order κ^2, we get a correction to the 2 point function. First, we note that

$$\langle \delta\phi \rangle = \kappa \langle F(\chi_0) \rangle + \mathcal{O}(\kappa^3) \tag{61}$$

Let us shift away the unobservable zero mode, defining

$$\delta\phi = f + \langle \delta\phi \rangle \tag{62}$$

where $\langle \delta\phi \rangle \simeq \kappa \langle \chi_0 \rangle$. We then have a probability distribution

$$\mathcal{L}(f|\kappa) = \int D\chi_0 |\psi_\perp[\chi_0]|^2 P_G[f + \langle \delta\phi \rangle - \kappa F(\chi_0)], \tag{63}$$

the likelihood of measuring a fluctuation f given κ.

Let us define $P_{\chi_0}(k)$ by

$$\langle F(\chi_0)_{\mathbf{k}_1} F(\chi_0)_{\mathbf{k}_2} \rangle = \int D\chi_0 |\psi_\perp[\chi_0]|^2 F(\chi_0)_{\mathbf{k}_1} F(\chi_0)_{\mathbf{k}_2} \equiv P_{\chi_0}(k_1)\delta(\mathbf{k}_1 + \mathbf{k}_2). \tag{64}$$

Expanding the likelihood in κ, we find

$$\mathcal{L}(f|\kappa) = \mathcal{L}(f|0) \left(1 + \frac{1}{2}\kappa^2 \int d\mathbf{k} \frac{P_{\chi_0}(k)}{P_{\delta\phi}(k)^2} f_{\mathbf{k}} f_{-\mathbf{k}} + \dots \right) \tag{65}$$

with

$$\mathcal{L}(f|0) = \exp\left(-\frac{1}{2} \int d\mathbf{k} \frac{1}{P_{\delta\phi}(k)} f_{\mathbf{k}} f_{-\mathbf{k}} \right) \tag{66}$$

At order κ^2, this simply means

$$P_{\delta\phi}(k) \to P_{\delta\phi}(k) + \kappa^2 P_{\chi_0}(k) \tag{67}$$

The χ sector modifies the power spectrum at order κ^2.

In the regime we are focused on, with couplings satisfying $\lambda n_e^2 \geq 1$, the function $P_{\chi_0}(k)$ will have a fully nonlinear dependence on $\log(k)$. In other words, it will not be a simple perturbative expansion in tilt, running, etc., in contrast to minimal single-field slow roll inflationary models. In the absence of non-Gaussianity, this could potentially provide an upper bound on κ of order

$$\Delta\kappa|_{2pf} \sim \frac{1}{N_P^{1/4}} \sqrt{\frac{P_{\delta\phi}}{P_{\chi_0}}} \tag{68}$$

which in itself is an improvement over the bound from the bispectrum constraint on $f_{\rm NL}^{\rm local}$, which scales like $N_{\rm p}^{-1/6}$ in this regime. Conversely, there is a similar improvement in the discovery potential in the two point function given (68).

5.2.2 Information in the tail for a family of models

Here we analyze the Non-Gaussian histogram quantitatively for the family of models defined in (59). Although the factorial enhancement of connected N point functions is general, the accessible information beyond the 2 point function is model-dependent. We will classify the regimes according to the behavior of the histogram and the various N point functions. (Even the 2 point function is informative, especially for theories with $\lambda n_e^2 > 1$, as there is no suppression of the running versus the tilt and so on.)

Analytic estimates for the size of the tail

Before getting into detailed analysis, we can estimate the size of the tail at the upper bound on κ that could be inferred from a bound on corrections to the 2-point function. Let us consider the class of models described above (59). For these, we can write the histogram as

$$\begin{aligned} \langle N_{\delta\hat{\phi}} \rangle &= \int d\chi_0 \, \mathcal{N}_{eq} \exp(-4\pi^2 \mu^{4-p} |\chi_0|^p / 3H^4) \frac{\exp(-(\delta\hat{\phi} + \kappa H (\chi_0/H)^m)^2 / 2\sigma^2)}{\sqrt{2\pi}\sigma} \, , \\ &= \int d\tilde{\chi}_0 \, \tilde{\mathcal{N}}_{eq} \exp(-|\tilde{\chi}_0|^p) \frac{\exp(-(\delta\hat{\phi} + \tilde{\kappa} H \tilde{\chi}_0^m)^2 / 2\sigma^2)}{\sqrt{2\pi}\sigma} \end{aligned} \tag{69}$$

where the only parameter that enters is

$$\tilde{\kappa} = \frac{\kappa}{(\mu (4\pi^2/3)^{1/(4-p)} / H)^{m(4-p)/p}} \tag{70}$$

To estimate the size of the tail, we use the relations

$$\tilde{\chi}_{0,tail}^m \sim \frac{\delta\hat{\phi}/H}{\tilde{\kappa}} \sim \frac{\tilde{\chi}_{0,tail}^{p/2}}{\tilde{\kappa}} \tag{71}$$

The first relation here is (30), and the second is the crossover between the dominance of the Gaussian in $\delta\hat{\phi}$ and the dominance of the tail, $\sim \exp(-\tilde{\chi}^p)$. Putting these together, we have a suppression of the tail by a factor

$$\exp(-\frac{1}{\tilde{\kappa}^{p/(m-p/2)}}) \tag{72}$$

In this section, we will imagine that we have observational access to all N point functions, and work out the information content of the tail versus low point correlators. In [17] we focused on an application to PBH formation, which is specifically sensitive to the tail (although even in that context, the variance can play a role as in [35]).

In that spirit, if we evaluate $\tilde{\kappa}$ at the bound it is possible to obtain from the 2 point function

$$\tilde{\kappa}^2 \frac{\Gamma(\frac{1+2m}{p})}{\Gamma(\frac{1}{p})} < \frac{1}{\sqrt{N_P}} \tag{73}$$

this scales like

$$\exp\{-N_P^{p/(4(m-p/2))} \left(\frac{\Gamma(\frac{1+2m}{p})}{\Gamma(\frac{1}{p})}\right)^{p/(2m-p)}\} \tag{74}$$

For the special model described around (36), we effectively have $p = 2, m = 2$. (In this case, we are not working with the equilbrium Starobinsky distribution, but the model is equivalent to the one with these values of p and m.) With $N_P = N_{pix} \sim 10^6$, this evaluates to $\exp(-\sqrt{N_{pix}}\Gamma(5/2)/\Gamma(1/2)) \simeq 10^{-326}$, hence nowhere near observable in the CMB. But relatively small changes in parameters make a big difference; larger m (e.g. of order 10) leads to much less suppression. Formally, smaller values of p would also do this, but dialing p in that way introduces the need to satisfy (29).

For the analysis in this section, we will illustrate the information content by considering different ratios of p/m. This captures the effect of dialing up the parameter m, which is motivated by the fact that large m matches onto the natural model (60) on a hyperbolic field space geometry.

Numerical analysis

Here, we construct realizations of the Non-Gaussian distributions discussed in the above section. We evaluate whether low point correlation functions are in principle best for detecting them, or whether instead other aspects of the distribution such as the tail or higher point correlators contain more information.

For the purposes of this section, we will use the following family of distributions:

$$P(-\infty < \phi < \infty) = \frac{1}{2\sqrt{2\pi}\Gamma\left(\frac{1}{p}+1\right)} \int_{-\infty}^{\infty} d\chi \exp\left(-|\chi|^p - \frac{(\phi - k^{\frac{1}{p}}\chi^m)^2}{2}\right) \tag{75}$$

The relation between k and $\tilde{\kappa} \propto k^{1/p}$ can be read off from (69) above. With this normalized distribution and a numerical analysis, we will check the estimates made above for models with accessible information on the tail.

If we focus for simplicity on N-point functions, we can determine which N would be best for detecting the non-Gaussianity. We generate a large number of Gaussian and non-Gaussian realizations (data sets), each containing N_P points. We evaluate the even N-point function estimator on each simulated map. For each N, we find the range in which 90% of the Gaussian results fall, starting from zero. In other words, for each correlation function, we find where the 90th percentile lies in the Gaussian realizations. We then compute the percentage of Non-Gaussian realizations that are above that 90th percentile. For tail-dominated models, such as the hyperbolic model (60), this can be a large percentage as we will see in an example below. We also do this for the likelihood.

To be more specific, we consider the following estimators for the N-point functions:

$$\hat{\mathcal{E}}_N = \frac{1}{N_P} \sum_{i=1}^{N_P} \phi_i^N \tag{76}$$

where ϕ_i are the N_P data points drawn from either a Gaussian or a Non-Gaussian distribution. We can also define an estimator by evaluating the log-likelihood on the map as follows:

$$\hat{\mathcal{E}}_L = \sum_{i=1}^{N_P} \log\left(\frac{P_{NG}(\phi_i)}{P_G(\phi_i)}\right) \tag{77}$$

The relative entropies are just the expectation values of this estimator over the two distributions:

$$\langle S\rangle_{NG} \equiv E[\hat{\mathcal{E}}_L]_{NG} = \int dx P_{NG}(x) \log\left(\frac{P_{NG}(x)}{P_G(x)}\right) \tag{78}$$

$$\langle S\rangle_{G} \equiv -E[\hat{\mathcal{E}}_L]_{G} = -\int dx P_{G}(x) \log\left(\frac{P_{NG}(x)}{P_G(x)}\right) \tag{79}$$

If we Taylor expand around $\kappa = 0$ in our distributions, the first surviving term is of order $N_P\kappa^4$, matching the two point function constraint. One can compare this to the full relative entropy, computed with respect to either the Gaussian or non-Gaussian probability. If these do not agree, then this indicates that the 2 point correlation function does not contain all the information.

As was discussed in the above section, the dominance of the tail is very sensitive to model parameters. As one particular example, we expect the distribution with $m = 3$ and $p = 0.7$ to be tail dominated. Figure 2 shows the results of the first 10 even N-pt functions for that particular distribution, with $k = 1/6$. The dashed line is the result of using the likelihood as our observable. Clearly, the 2-pt function does not do a good job of detecting the Non-Gaussianity. The optimal N-pt functions are the 6-th and the 8-th in this case. Conversely, in a non-tail dominated model, the 2-pt function would essentially be lying on the

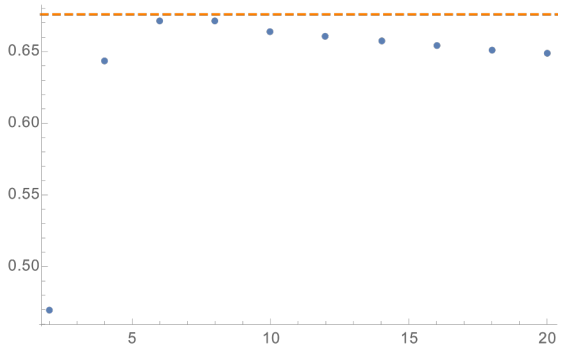

Figure 2: The horizontal axis is the even N-pt functions up to $N = 20$ for the distribution with $m = 3$ and $p = 0.7$, with $N_P = 1000$. The vertical axis is the fraction of samples that are above the 90th percentile of those in the Gaussian distribution as described in the text. The dashed line is the likelihood. The low point correlators are not optimal in this example.

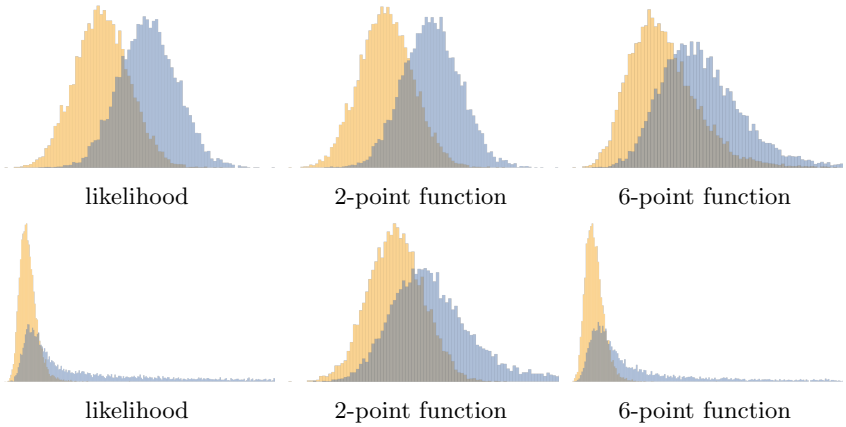

Figure 3: The likelihood and the distributions of the 2-point function and 6-point function estimators, for the Gaussian distribution (in yellow), and a non-Gaussian distribution (in blue). The first row is the model with $m = 1$, $p = 4$, $k = 1/20$, $N_P = 1000$ and the second row with $m = 3$, $p = 0.7$, $k = 1/6$, $N_P = 1000$.

m	p	k	$\langle S \rangle_G$	$\langle S \rangle_{NG}$	Best N-pf
1	1/16	1/29	0.86	73	8-12
1	1/8	1/17	0.86	35	6-10
1	1/4	1/10	1.1	5.8	4-6
1	1/2	1/6	1.9	2.5	2-4
1	1	1/5	1.4	1.5	2
1	4	1/20	1.3	1.4	2
3	0.7	1/6	1.0	13.7	6-8

Table 1: Numerical results for different distributions with $N_P = 1000$ and 10000 samples. S is the relative entropy, computed either with respect to the Gaussian or Non-Gaussian distribution as indicated in the columns, including the factor of N_P. We chose this to be order 1, i.e. a barely detectable difference between the two distributions, according to the Gaussian-weighted relative entropy. For tail-dominated models, we find a discrepancy between the two relative entropies, with a large relative entropy weighted with the non-Gaussian distribution.

likelihood line with the successive N-pt functions decreasing and plateauing for large N.

In Figure 3 the distribution of the likelihood, 2-pt function and 6-pt function are plotted. For the case with $m = 1$ and $p = 4$, the 2-pt function distribution is essentially the same as the likelihood, while the 6-pt function has a significantly more tailed distribution. This non-Gaussian distribution of the estimator illustrates why the naive signal/noise analyzed in section 5.1 – which is generically factorial enhanced – is not by itself an indicator of observational sensitivity. However, in the $m = 3$ and $p = 0.7$ model, the 2-pt function is very different from the likelihood. This behavior is model-dependent, but applies to interesting models such as (60).

Our results for different parameters are summarized in Table 1. The results for models with $m \neq 1$ and p are similar to those with $m = 1$ and $p' = \frac{p}{m}$, and a large ratio of m/p should be a good guide to the natural hyperbolic model (60) [17].

6 Conclusions and future directions

In this work, we showed that in the multifield inflationary context, factorial enhancement of N point correlation functions survives quantum effects and applies in the regime of kinematic interest. This is a basic question in quantum field theory motivated by the factorial enhancement known in particular parameter and kinematic regimes. It is simpler to analyze more fully and exploit in the regime of physical interest in our cosmological setting than in collider physics (although in that context this question has stimulated a number of interesting results [1][2] [3] [4] [5][7]). The basic reason for this is the dilution of gradients, along with the calculably stochastic behavior of the system that applies in some

regimes of couplings.

Specifically, we derived and applied the enhanced amplitude of these large N-point functions in the study of primordial non-Gaussianity. We encountered some subtleties along the way, but were left with interesting model-dependent possibilities for substantially enhanced sensitivity beyond low point correlators. It would be interesting to explore in more depth the phenomenological implications, beyond that of enhanced primordial black hole production addressed recently in [17].

The models we analyzed in this work contain additional fields during inflation, which is reasonable given the multiple fields in the Standard model as well as hidden sectors that often arise in string theory. This enabled us to apply the theory of stochastic inflation for certain windows of couplings, as well as mixing interactions among field sectors in all cases. A natural question that arises is whether this effect persists in the case when any additional fields are too heavy during inflation to have such effects, reducing the system effectively to a single-field model of the primordial perturbations. We leave these questions to future work, perhaps building from recent progress on the calculation of multipoint correlators in other areas of quantum field theory [7]. In the present work, the kinematic simplicity and resulting calculability of the ultralocal multifield dynamics in early universe inflation enabled us to settle the factorial enhancement question in the affirmative in this context.

Acknowledgments We thank Mehrdad Mirbabayi, Leonardo Senatore, and Matias Zaldarriaga for extensive discussions and collaboration on this subject. We also thank N. Arkani-Hamed, J. R. Bond, J. Cardy, P. Creminelli, R. Flauger, V. Gorbenko, Z. Komargodski, M. Munchmeyer, D. Murli, J. Polchinski, S. Shenker, K. Smith, D. Spergel, J. Thompson, and B. Wandelt for useful related discussions. This research was supported in part by the Simons Foundation Origins of the Universe Initiative (modern inflationary cosmology collaboration), and by a Simons Investigator award. GP and ES are grateful to the KITP for hospitality during part of this project.

References

[1] M. B. Voloshin, "Multiparticle production in lambda-phi**4 theory with weak coupling," TPI-MINN-92-27-T.

[2] L. S. Brown, "Summing tree graphs at threshold," Phys. Rev. D **46**, R4125 (1992) doi:10.1103/PhysRevD.46.R4125 [hep-ph/9209203].

[3] E. N. Argyres, R. H. P. Kleiss and C. G. Papadopoulos, "Cross-section estimates for multi - Higgs production at high-energies," Nucl. Phys. B **391**, 57 (1993). doi:10.1016/0550-3213(93)90141-B

E. N. Argyres, R. H. P. Kleiss and C. G. Papadopoulos, "Multiscalar amplitudes to all orders in perturbation theory," Phys. Lett. B **308**, 292

(1993) Addendum: [Phys. Lett. B **319**, 544 (1993)] doi:10.1016/0370-2693(93)91287-W [hep-ph/9303321].

[4] D. T. Son, "Semiclassical approach for multiparticle production in scalar theories," Nucl. Phys. B **477**, 378 (1996) doi:10.1016/0550-3213(96)00386-0 [hep-ph/9505338].

M. V. Libanov, V. A. Rubakov, D. T. Son and S. V. Troitsky, "Exponentiation of multiparticle amplitudes in scalar theories," Phys. Rev. D **50**, 7553 (1994) doi:10.1103/PhysRevD.50.7553 [hep-ph/9407381].

[5] V. V. Khoze, "Multiparticle production in the large λn limit: realising Higgsplosion in a scalar QFT," JHEP **1706**, 148 (2017) doi:10.1007/JHEP06(2017)148 [arXiv:1705.04365 [hep-ph]].

V. V. Khoze and M. Spannowsky, "Higgsplosion: Solving the Hierarchy Problem via rapid decays of heavy states into multiple Higgs bosons," arXiv:1704.03447 [hep-ph].

[6] S. Ghosh and S. Raju, "Breakdown of String Perturbation Theory for Many External Particles," Phys. Rev. Lett. **118**, no. 13, 131602 (2017) doi:10.1103/PhysRevLett.118.131602 [arXiv:1611.08003 [hep-th]].

S. Ghosh and S. Raju, "Loss of locality in gravitational correlators with a large number of insertions," arXiv:1706.07424 [hep-th].

[7] A. Bourget, D. Rodriguez-Gomez and J. G. Russo, "A limit for large R-charge correlators in $\mathcal{N} = 2$ theories," JHEP **1805**, 074 (2018) doi:10.1007/JHEP05(2018)074 [arXiv:1803.00580 [hep-th]].

A. Monin, "Inconsistencies of higgsplosion," arXiv:1808.05810 [hep-th].

A. Grassi, Z. Komargodski and L. Tizzano, "Extremal Correlators and Random Matrix Theory," arXiv:1908.10306 [hep-th].

G. Badel, G. Cuomo, A. Monin and R. Rattazzi, "Feynman diagrams and the large charge expansion in $3-\varepsilon$ dimensions," Phys. Lett. B **802**, 135202 (2020) doi:10.1016/j.physletb.2020.135202 [arXiv:1911.08505 [hep-th]].

G. Arias-Tamargo, D. Rodriguez-Gomez and J. G. Russo, "The large charge limit of scalar field theories and the Wilson-Fisher fixed point at $\epsilon = 0$," JHEP **1910**, 201 (2019) doi:10.1007/JHEP10(2019)201 [arXiv:1908.11347 [hep-th]].

G. Badel, G. Cuomo, A. Monin and R. Rattazzi, "The Epsilon Expansion Meets Semiclassics," JHEP **1911**, 110 (2019) doi:10.1007/JHEP11(2019)110 [arXiv:1909.01269 [hep-th]].

M. Watanabe, "Accessing Large Global Charge via the ϵ-Expansion," arXiv:1909.01337 [hep-th].

M. Dine, H. H. Patel and J. F. Ulbricht, "Behavior of Cross Sections for Large Numbers of Particles," arXiv:2002.12449 [hep-ph].

[8] S. Hellerman, D. Orlando, S. Reffert and M. Watanabe, "On the CFT Operator Spectrum at Large Global Charge," JHEP **1512**, 071 (2015) doi:10.1007/JHEP12(2015)071 [arXiv:1505.01537 [hep-th]].

S. Hellerman, N. Kobayashi, S. Maeda and M. Watanabe, "A Note on Inhomogeneous Ground States at Large Global Charge," JHEP **1910**, 038 (2019) doi:10.1007/JHEP10(2019)038 [arXiv:1705.05825 [hep-th]].

S. Hellerman and S. Maeda, "On the Large R-charge Expansion in $\mathcal{N} = 2$ Superconformal Field Theories," JHEP **1712**, 135 (2017) doi:10.1007/JHEP12(2017)135 [arXiv:1710.07336 [hep-th]].

J. Polchinski and E. Silverstein, "Large-density field theory, viscosity, and '$2k_F$' singularities from string duals," Class. Quant. Grav. **29**, 194008 (2012) doi:10.1088/0264-9381/29/19/194008 [arXiv:1203.1015 [hep-th]].

[9] D. Babich, P. Creminelli and M. Zaldarriaga, "The Shape of non-Gaussianities," JCAP **0408**, 009 (2004) doi:10.1088/1475-7516/2004/08/009 [astro-ph/0405356].

[10] P. A. R. Ade *et al.* [Planck Collaboration], "Planck 2015 results. XVII. Constraints on primordial non-Gaussianity," Astron. Astrophys. **594**, A17 (2016) doi:10.1051/0004-6361/201525836 [arXiv:1502.01592 [astro-ph.CO]].

P. A. R. Ade *et al.* [Planck Collaboration], "Planck 2015 results. XVI. Isotropy and statistics of the CMB," Astron. Astrophys. **594**, A16 (2016) doi:10.1051/0004-6361/201526681 [arXiv:1506.07135 [astro-ph.CO]].

Bennett, C.L., et.al., "Nine-Year Wilkinson Microwave Anisotropy Probe (WMAP) Observations: Final Maps and Results" The Astrophysical Journal Supplement, Volume 208, Issue 2, article id. 20, 54 pp. (2013).

[11] D. S. Salopek and J. R. Bond, "Nonlinear evolution of long wavelength metric fluctuations in inflationary models," Phys. Rev. D **42**, 3936 (1990). doi:10.1103/PhysRevD.42.3936

[12] A. A. Starobinsky and J. Yokoyama, "Equilibrium state of a selfinteracting scalar field in the De Sitter background," Phys. Rev. D **50**, 6357 (1994) doi:10.1103/PhysRevD.50.6357 [astro-ph/9407016].

A. A. Starobinsky, "Stochastic De Sitter (inflationary) Stage In The Early Universe," Lect. Notes Phys. **246**, 107 (1986). *doi* : $10.1007/3 - 540 - 16452 - 9_6$

H. Collins, R. Holman and T. Vardanyan, "The quantum Fokker-Planck equation of stochastic inflation," JHEP **1711**, 065 (2017) doi:10.1007/JHEP11(2017)065 [arXiv:1706.07805 [hep-th]].

V. Vennin and A. A. Starobinsky, "Correlation Functions in Stochastic Inflation," Eur. Phys. J. C **75** (2015) 413 doi:10.1140/epjc/s10052-015-3643-y [arXiv:1506.04732 [hep-th]].

[13] V. Gorbenko and L. Senatore, "$\lambda\phi^4$ in dS," arXiv:1911.00022 [hep-th].

[14] R. Flauger, M. Mirbabayi, L. Senatore and E. Silverstein, "Productive Interactions: heavy particles and non-Gaussianity," arXiv:1606.00513 [hep-th].

M. Münchmeyer and K. M. Smith, "Higher N-point function data analysis techniques for heavy particle production and WMAP results," Phys. Rev. D **100**, no. 12, 123511 (2019) doi:10.1103/PhysRevD.100.123511 [arXiv:1910.00596 [astro-ph.CO]].

[15] J. R. Bond, A. V. Frolov, Z. Huang and L. Kofman, "Non-Gaussian Spikes from Chaotic Billiards in Inflation Preheating," Phys. Rev. Lett. **103**, 071301 (2009) doi:10.1103/PhysRevLett.103.071301 [arXiv:0903.3407 [astro-ph.CO]].

[16] V. Demozzi, A. Linde and V. Mukhanov, "Supercurvaton," JCAP **1104**, 013 (2011) doi:10.1088/1475-7516/2011/04/013 [arXiv:1012.0549 [hep-th]].

[17] G. Panagopoulos and E. Silverstein, "Primordial Black Holes from non-Gaussian tails," arXiv:1906.02827 [hep-th].

[18] L. Leblond and E. Pajer, "Resonant Trispectrum and a Dozen More Primordial N-point functions," JCAP **1101**, 035 (2011) doi:10.1088/1475-7516/2011/01/035 [arXiv:1010.4565 [hep-th]].

[19] X. Chen, G. A. Palma, W. Riquelme, B. Scheihing Hitschfeld and S. Sypsas, "Landscape tomography through primordial non-Gaussianity," Phys. Rev. D **98**, no. 8, 083528 (2018) doi:10.1103/PhysRevD.98.083528 [arXiv:1804.07315 [hep-th]].

X. Chen, G. A. Palma, B. Scheihing Hitschfeld and S. Sypsas, "Reconstructing the Inflationary Landscape with Cosmological Data," Phys. Rev. Lett. **121**, no. 16, 161302 (2018) doi:10.1103/PhysRevLett.121.161302 [arXiv:1806.05202 [astro-ph.CO]].

[20] M. LoVerde, E. Nelson and S. Shandera, "Non-Gaussian Mode Coupling and the Statistical Cosmological Principle," JCAP **1306**, 024 (2013) doi:10.1088/1475-7516/2013/06/024 [arXiv:1303.3549 [astro-ph.CO]].

[21] P. Hintz and A. Vasy, "The global non-linear stability of the Kerr-de Sitter family of black holes," arXiv:1606.04014 [math.DG].

[22] J. M. Maldacena, "Non-Gaussian features of primordial fluctuations in single field inflationary models," JHEP **0305**, 013 (2003) doi:10.1088/1126-6708/2003/05/013 [astro-ph/0210603].

[23] M. Alishahiha, E. Silverstein and D. Tong, "DBI in the sky," Phys. Rev. D **70**, 123505 (2004) doi:10.1103/PhysRevD.70.123505 [hep-th/0404084].

[24] C. Cheung, P. Creminelli, A. L. Fitzpatrick, J. Kaplan and L. Senatore, "The Effective Field Theory of Inflation," JHEP **0803**, 014 (2008) doi:10.1088/1126-6708/2008/03/014 [arXiv:0709.0293 [hep-th]].

X. Chen, M. x. Huang, S. Kachru and G. Shiu, "Observational signatures and non-Gaussianities of general single field inflation," JCAP **0701**, 002 (2007) doi:10.1088/1475-7516/2007/01/002 [hep-th/0605045].

C. Cheung, A. L. Fitzpatrick, J. Kaplan and L. Senatore, "On the consistency relation of the 3-point function in single field inflation," JCAP **0802** (2008) 021 doi:10.1088/1475-7516/2008/02/021 [arXiv:0709.0295 [hep-th]].

[25] T. J. Allen, B. Grinstein and M. B. Wise, "Nongaussian Density Perturbations in Inflationary Cosmologies," Phys. Lett. B **197**, 66 (1987). doi:10.1016/0370-2693(87)90343-1

M. Srednicki, "Cosmic variance of the three point correlation function of the cosmic microwave background," Astrophys. J. **416**, L1 (1993) doi:10.1086/187056 [astro-ph/9306012].

T. Falk, R. Rangarajan and M. Srednicki, "Dependence of density perturbations on the coupling constant in a simple model of inflation," Phys. Rev. D **46**, 4232 (1992) doi:10.1103/PhysRevD.46.4232 [astro-ph/9208002].

A. Gangui, F. Lucchin, S. Matarrese and S. Mollerach, "The Three point correlation function of the cosmic microwave background in inflationary models," Astrophys. J. **430**, 447 (1994) doi:10.1086/174421 [astro-ph/9312033].

A. D. Linde and V. F. Mukhanov, "Nongaussian isocurvature perturbations from inflation," Phys. Rev. D **56**, R535 (1997) doi:10.1103/PhysRevD.56.R535 [astro-ph/9610219].

E. Komatsu and D. N. Spergel, "Acoustic signatures in the primary microwave background bispectrum," Phys. Rev. D **63**, 063002 (2001) doi:10.1103/PhysRevD.63.063002 [astro-ph/0005036].

V. Acquaviva, N. Bartolo, S. Matarrese and A. Riotto, "Second order cosmological perturbations from inflation," Nucl. Phys. B **667**, 119 (2003) doi:10.1016/S0550-3213(03)00550-9 [astro-ph/0209156].

F. Bernardeau and J. P. Uzan, "NonGaussianity in multifield inflation," Phys. Rev. D **66**, 103506 (2002) doi:10.1103/PhysRevD.66.103506 [hep-ph/0207295].

N. Bartolo, S. Matarrese and A. Riotto, "Nongaussianity from inflation," Phys. Rev. D **65**, 103505 (2002) doi:10.1103/PhysRevD.65.103505 [hep-ph/0112261].

D. H. Lyth, C. Ungarelli and D. Wands, "The Primordial density perturbation in the curvaton scenario," Phys. Rev. D **67**, 023503 (2003) doi:10.1103/PhysRevD.67.023503 [astro-ph/0208055].

[26] A. D. Linde and V. Mukhanov, "The curvaton web," JCAP **0604**, 009 (2006) doi:10.1088/1475-7516/2006/04/009 [astro-ph/0511736].

L. Kofman, "Probing string theory with modulated cosmological fluctuations," astro-ph/0303614.

D. H. Lyth and D. Wands, "Generating the curvature perturbation without an inflaton," Phys. Lett. B **524**, 5 (2002) doi:10.1016/S0370-2693(01)01366-1 [hep-ph/0110002].

G. Dvali, A. Gruzinov and M. Zaldarriaga, "Cosmological perturbations from inhomogeneous reheating, freezeout, and mass domination," Phys. Rev. D **69**, 083505 (2004) doi:10.1103/PhysRevD.69.083505 [astro-ph/0305548].

G. Dvali, A. Gruzinov and M. Zaldarriaga, "A new mechanism for generating density perturbations from inflation," Phys. Rev. D **69**, 023505 (2004) doi:10.1103/PhysRevD.69.023505 [astro-ph/0303591].

M. Zaldarriaga, "Non-Gaussianities in models with a varying inflaton decay rate," Phys. Rev. D **69**, 043508 (2004) doi:10.1103/PhysRevD.69.043508 [astro-ph/0306006].

[27] W. E. East, M. Kleban, A. Linde and L. Senatore, "Beginning inflation in an inhomogeneous universe," JCAP **1609**, no. 09, 010 (2016) doi:10.1088/1475-7516/2016/09/010 [arXiv:1511.05143 [hep-th]].

[28] M. Kleban and L. Senatore, "Inhomogeneous Anisotropic Cosmology," JCAP **1610** (2016) no.10, 022 doi:10.1088/1475-7516/2016/10/022 [arXiv:1602.03520 [hep-th]].

[29] X. Dong, B. Horn, E. Silverstein and A. Westphal, "Simple exercises to flatten your potential," Phys. Rev. D **84**, 026011 (2011) doi:10.1103/PhysRevD.84.026011 [arXiv:1011.4521 [hep-th]].

[30] L. McAllister, E. Silverstein, A. Westphal and T. Wrase, "The Powers of Monodromy," JHEP **1409**, 123 (2014) doi:10.1007/JHEP09(2014)123 [arXiv:1405.3652 [hep-th]].

[31] A. J. Tolley and M. Wyman, "Stochastic Inflation Revisited: Non-Slow Roll Statistics and DBI Inflation," JCAP **0804**, 028 (2008) doi:10.1088/1475-7516/2008/04/028 [arXiv:0801.1854 [hep-th]].

[32] R. Kallosh, A. Linde and D. Roest, "Large field inflation and double α-attractors," JHEP **1408**, 052 (2014) doi:10.1007/JHEP08(2014)052 [arXiv:1405.3646 [hep-th]].

[33] P. Creminelli, L. Senatore and M. Zaldarriaga, "Estimators for local non-Gaussianities," JCAP **0703**, 019 (2007) doi:10.1088/1475-7516/2007/03/019 [astro-ph/0606001].

M. Kamionkowski, T. L. Smith and A. Heavens, "The CMB Bispectrum, Trispectrum, non-Gaussianity, and the Cramer-Rao Bound," Phys. Rev.

D **83**, 023007 (2011) doi:10.1103/PhysRevD.83.023007 [arXiv:1010.0251 [astro-ph.CO]].

T. L. Smith, M. Kamionkowski and B. D. Wandelt, "The Probability Distribution for Non-Gaussianity Estimators," Phys. Rev. D **84**, 063013 (2011) doi:10.1103/PhysRevD.84.063013 [arXiv:1104.0930 [astro-ph.CO]].

T. L. Smith, D. Grin and M. Kamionkowski, "Improved estimator for non-Gaussianity in cosmic microwave background observations," Phys. Rev. D **87**, 063003 (2013) doi:10.1103/PhysRevD.87.063003 [arXiv:1211.3417 [astro-ph.CO]].

N. Kogo and E. Komatsu, "Angular trispectrum of cmb temperature anisotropy from primordial non-gaussianity with the full radiation transfer function," Phys. Rev. D **73**, 083007 (2006) doi:10.1103/PhysRevD.73.083007 [astro-ph/0602099].

T. Okamoto and W. Hu, "The angular trispectra of CMB temperature and polarization," Phys. Rev. D **66**, 063008 (2002) doi:10.1103/PhysRevD.66.063008 [astro-ph/0206155].

[34] R. Kallosh and A. Linde, "Escher in the Sky," Comptes Rendus Physique **16**, 914 (2015) doi:10.1016/j.crhy.2015.07.004 [arXiv:1503.06785 [hep-th]].

A. R. Brown, "Hyperbolic Inflation," Phys. Rev. Lett. **121**, no. 25, 251601 (2018) doi:10.1103/PhysRevLett.121.251601 [arXiv:1705.03023 [hep-th]].

[35] T. Nakama, B. Carr and J. Silk, "Limits on primordial black holes from μ distortions in cosmic microwave background," Phys. Rev. D **97**, no. 4, 043525 (2018) doi:10.1103/PhysRevD.97.043525 [arXiv:1710.06945 [astro-ph.CO]].

T. Nakama, T. Suyama and J. Yokoyama, "Supermassive black holes formed by direct collapse of inflationary perturbations," Phys. Rev. D **94**, no. 10, 103522 (2016) doi:10.1103/PhysRevD.94.103522 [arXiv:1609.02245 [gr-qc]].